



HAL
open science

Fire resistance of carbon-based composite materials under both ideal and realistic normative configurations

N. Grange, B. Manescau, K. Chetehouna, N. Gascoin, L. Lamoot, A. Coppalle, S. Senave, I. Reynaud

► To cite this version:

N. Grange, B. Manescau, K. Chetehouna, N. Gascoin, L. Lamoot, et al.. Fire resistance of carbon-based composite materials under both ideal and realistic normative configurations. Applied Thermal Engineering, 2019, 159, pp.113834 -. 10.1016/j.applthermaleng.2019.113834 . hal-03485882

HAL Id: hal-03485882

<https://hal.science/hal-03485882>

Submitted on 20 Dec 2021

HAL is a multi-disciplinary open access archive for the deposit and dissemination of scientific research documents, whether they are published or not. The documents may come from teaching and research institutions in France or abroad, or from public or private research centers.

L'archive ouverte pluridisciplinaire **HAL**, est destinée au dépôt et à la diffusion de documents scientifiques de niveau recherche, publiés ou non, émanant des établissements d'enseignement et de recherche français ou étrangers, des laboratoires publics ou privés.



Distributed under a Creative Commons Attribution - NonCommercial 4.0 International License

Fire resistance of carbon-based composite materials under both ideal and realistic normative configurations

N. Grange^{1*}, B. Manescau¹, K. Chetehouna¹, N. Gascoin¹, L. Lamoot¹, A. Coppalle², S. Senave³, I. Reynaud³

¹INSA Centre Val de Loire, Univ. Orléans, PRISME EA 4229, F-18022 Bourges, France

²CNRS UMR 6614 CORIA, INSA de Rouen, 76800 St Etienne du Rouvray, France

³DAHER, 41400 St Julien de Chédon, France

*Corresponding author: nathan.grange@insa-cvl.fr

Keywords: Fire resistant materials, NexGen Burner, Cone calorimeter, Multiscale analysis, Infrared visualization.

Highlights:

- Fire behavior of three carbon reinforced composites samples is evaluated for two significant scales
- The FAA standard NexGen burner is used to evaluate the fire resistance at large scale
- Experimental mass loss demonstrates the superior thermal stability of carbon-PEKK
- No open plies are observed after fire exposure of Carbon-BMI samples

Abstract

In industrial and transportation systems, composite materials are now commonly used. However, despite their superior mechanical properties and weight reduction capacity, such materials are highly vulnerable to fire. To assess such risks in the aeronautical industry, standard tests are performed at different scales on representative selected samples. In this work, the fire behavior of three different carbon-reinforced composites (Carbon-phenolic, Carbon-PEKK and Carbon-BMI) is evaluated at medium and large-scale using state-of-the-art techniques, such as Cone calorimeter and NexGen burner. To provide a detailed description of the fire behavior of these three materials, mass loss as well as the backward face temperature are provided and compared for the different scales. The results highlight better thermal

stability of the carbon-PEKK and the carbon-BMI in comparison with the carbon-phenolic; moreover the evolution of the phenomena between different scales is observed.

1. Introduction

In the aerospace industry, composite materials profoundly improved the design of aircraft due to their main advantages in weight reduction, [1] and strong mechanical properties [2] allowing significant cost reductions. Nevertheless, these materials also present many advantages in every modern transportation systems, such as trains [3], planes [4], automobiles [5] and even bicycles [6]. However, the quest of utilizing composite materials in modern transport system is still in its infancy due to being vulnerable when exposed to fire or even high temperatures. Unfortunately, during their thermal degradation, composite materials serve as a fuel and also produce toxic fumes resulting in an explosive atmosphere. Thus, fire spread might continue even after the original source of fire is extinguished or depleted [7].

To address these issues, various experiments involving composite materials were performed at different scales to understand, to predict and to certify their behavior when they are exposed to fire [8]. Particularly, in the aerospace industry, materials have to achieve standard fire tests at large scale; following rules such as ISO 2685 [9] or FAA AC 20-135 [10]. These tests, which involve flat panels or even complex airplane parts, aim at ensuring that every constitutive element of the aircraft retain their function for the longest time possible to guarantee the safety of passengers or carried goods.

Indeed, composite materials, in addition to their mechanical duty, are used to provide a fire protection in aeronautics. The constant evolution of fire safety standards has raised the bars for composite materials. Thus, to guarantee good protection from fire, these materials must sustain fire as long as possible with low amount of fume production to allow passenger to evacuate safely.

In the present work, the fire behavior is experimentally investigated at two different scales. At meso-scale (samples about 10 cm×10cm) a cone calorimeter (radiative heating) device is used, which is frequently employed to assess the fire behavior of composite materials estimating heat release rate [11], flammability [12] or fire performances [13]. Moreover, this kind of test is considered as a standard test for materials [14] providing a realistic degradation environment (heat flux ranges from 30 to 120 kW/m²). It provides Heat Release Rate (HRR), surface temperature and Mass Loss Rate (MLR), which are the required parameters to evaluate the fire behavior of composite materials; for example, MLR is one of the most important factors as it is directly linked to the pyrolysis rate, and represents the initial cause of the combustion process [15]. At large scale, a NexGen Burner (designed by the FAA) as per the aeronautical standards with a kerosene flame is used [9, 10] to test samples (about 50 cm×50 cm) which are representatives of parts of aircraft structures. By comparing the results obtained from these two scales, the relevance of tested materials at different scales are evaluated and the degradation behavior of tested specimens using the two different heat sources is compared (i.e. radiative heat flux and kerosene flame). . Therefore, to contribute to the ongoing work on the assessment of fire behavior of composite materials at the above-mentioned two different scales, the fire behavior of three carbon-reinforced composites cured from pre-impregnated fibers are studied. The first is a thermosetting phenolic, which finds multiple applications in the industry for thermal protection, especially in the aerospace industry [7]; moreover, it is also used for automotive components or fire barriers in offshore oil platform [16]. Under fire conditions, carbon-phenolic composites are characterized by a high yield of char (up to 50% of the initial mass) and a low thermal conductivity [17] involving a slow ignition time and an easy extinguishment [18] due to moderate number of volatiles yield and reduced flammability [19]. Previous work done in this domain demonstrates that degradation of the carbon-phenolic is driven by two reactions under inert

atmosphere with respective mass loss of approximately 20 %, and by four reactions under oxidative atmosphere with complete depletion of materials at the end of test [20]. The thermal characterization of the carbon-phenolic composite also illustrates that this material has a high specific heat and reduced thermal conductivity at high temperature enhancing its ability to withstand fire [17].

The second is the thermosetting bismaleimide (BMI), originally developed for structural applications, these composites are known to be used where prolonged exposure to high temperature or enhanced fatigue resistance is necessary [19]. Although, the Bismaleimide (BMI) resin offers high mechanical and thermal performance for aerospace applications but their brittleness and vulnerability to impact and damage due to high cross-linking density has limited its effective utilization. However, after curing the maleimide groups, their high cross-linking density gets better which might result in a superior thermal stability with a melting temperature (T_m) between 300 and 350 °C and a glass transition temperature (T_g) between 150 and 250 °C [19]. Moreover, their composition, made of aromatic group and nitrogen ensures a low amount of volatiles emissions and a flame retardancy effect [19]. The thermogravimetric analysis of the BMI resin demonstrates that the resin pyrolysis occurs between 300 and 400 °C [24]. Moreover, it has been observed that under oxidative atmosphere (Air) this composite material loses about 10 to 20% by mass [24], showing a good thermal stability with low degradation.

Finally, the carbon-PEKK thermoplastic is studied, this thermoplastic polymer which is known for its high mechanical performance was originally designed for external structure and cabin interiors in aerospace as well as automotive industry [20] [21]. The monomer of PEKK resin is characterized by three aromatic groups in the main chain with ether and ketone linkages, providing high thermal stability, with a glass transition and a melting temperature of, $T_g = 156$ °C and a melting temperature (T_m) equal to 338 °C respectively [22]. Moreover,

the high yield of stable carbonaceous char during the decomposition process (~60% of initial mass) leads to a reduction in volatiles during combustion and display superior flammability resistance [23]. Thermogravimetric analysis at small scale demonstrates that the resin degradation starts at about 500 °C with a remaining mass loss of less than 20 %, whereas under oxidative atmosphere, no residual amount of materials was found and it presents three global reactions that are associated with the resin pyrolysis, char and carbon-fiber oxidation [22]. The carbon-PEKK decomposition is driven by one major reaction under inert atmosphere (resin pyrolysis) and three under oxidative atmospheres (resin pyrolysis, char and carbon-fibers oxidation). Moreover, the measurement of thermal properties confirms the higher thermal stability of the carbon-PEKK [17].

This study elaborates on a detailed description of this composite using a cone calorimeter and a NexGen burner for the first time. Finally, the experimental observations and results, such as the backward face temperatures, mass loss ratio and heat release rates support the scientific finding of the subject matter.

2. Material and methods

2.1. Materials Description

The three carbon-reinforced composites (cured using pre-impregnated fibers) studied in this work are manufactured and provided by the company DAHER. Among the three composites, two are thermosetting i.e. a carbon-BMI and a carbon-phenolic and one is thermoplastic carbon-PEKK. The two samples of thermoset considered in this work are a 6 plies carbon-BMI sample (1.5 mm in thickness) with a fiber mass fraction of 40 % and a 6 plies Carbon-phenolic (1.5 mm in thickness) with a fiber mass fraction of 42 %. Later, both thermosetting materials are compared to a 12 plies of thermoplastic carbon-PEKK (1.9 mm thickness) with a fiber mass fraction of 41%.

2.2. Cone calorimeter experiments

Based on the ISO 5660-1: 2002 standard [14], the meso-scale experiments are carried out using a cone calorimeter. A 10×10 cm sample with an exposed surface of 88.4 cm^2 was placed at 35 mm from a heat source under a constant heat flux of 100 kW/m^2 and measurements were recorded. The samples were placed horizontally and vertically to evaluate the result for both configurations (cf. Figure 1). To experiments are performed twice to ensure the reliability of the data obtained in this study. Moreover, the Mass Loss Rate (MLR), the Heat Release Rate (HRR) and the Backward Face Temperature (BFT) are measured while performing the experiments. In the vertical configuration the measure of the BFT is made using a Flir A600 infrared thermography apparatus which allowed to measure the temperature field on a zone of 40×40 mm located at the center of the backward face of the sample covered by a graphite layer (with a known emissivity of $\varepsilon = 0.95$). In the horizontal configuration, the MLR is measured using a balance situated under the sample holder. The HRR is determined using the oxygen depletion principle [25] based on the concentration of O_2 , CO and CO_2 . To this end, , smoke is absorbed at 24 l/s with a gas sampling of the combustion products at 58.3 ml/s . The HRR is estimated with a global uncertainty of 5 %, and with a confidence level of 95 %.

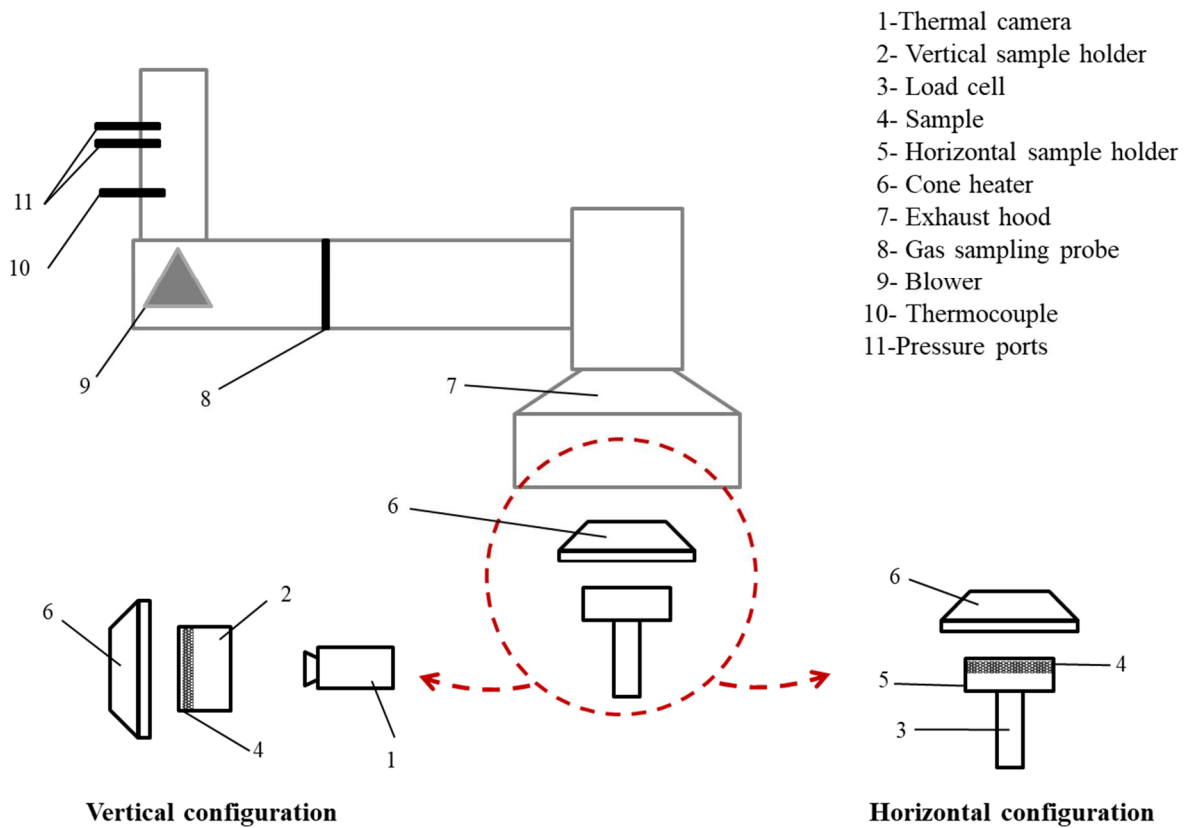


Figure 1. Overview of the cone calorimeter experiments.

2.3. NexGen Burner experiments

Large-scale experiments are conducted in accordance to the fire standards accepted in the aerospace industry (ISO 2685 and FAA AC20-135), using a next generation fire burner (NexGen Burner,) designed by the FAA, (see Figure 2). This kind of test bench has been designed for certifications and is a representative of realistic fire conditions, close to those encountered in real-life accidents, particularly in areas around aircraft engines. As mentioned in the standards, the samples must withstand a fire exposition of 15 minutes to a kerosene-air diffusion flame without igniting the material or self-ignition in the unexposed areas. The impinging flame must ensure a heat flux of $116 \text{ kW/m}^2 \pm 10 \text{ kW/m}^2$ and a mean flame temperature of $1100 \text{ }^\circ\text{C} \pm 80 \text{ }^\circ\text{C}$ [10].

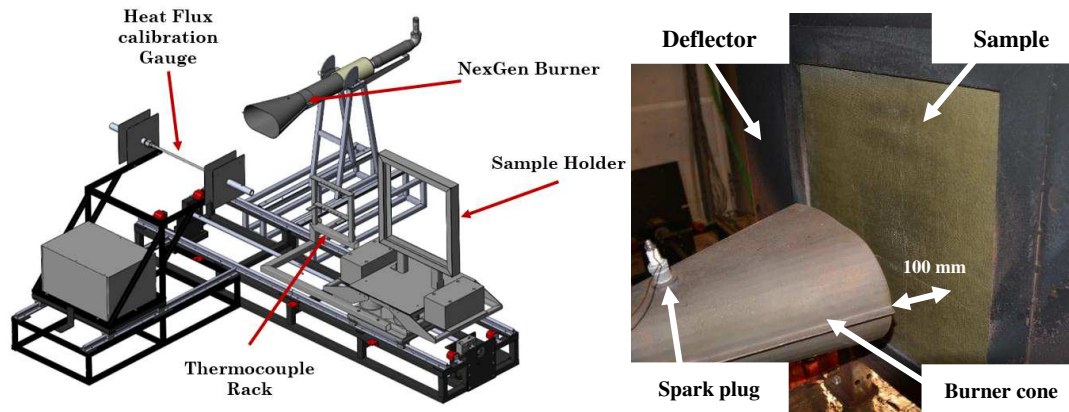


Figure 2. Overview of the NexGen Burner Test Bench.

These fire conditions are generated using a manually operated air supply circuit which is providing to the burner air pressure ranging from 1.90 bar to 4.5 bar generated with a compressor.. To ensure identical conditions for each run, the inlet temperature in the burner is stabilized between 5 and 15 ° C. The air is passed through a water exchanger allowing it to get cooled and then it is circulated in a coil stored in a freezer to stabilize the temperature, the air is then passed through a sonic throat providing a constant flow at atmospheric pressure at the outlet with limited pressure variations. The fuel used is Jet A-1 kerosene, which is vaporized into the burner cone using a Delavan injector with a temperature between 0 and 10 °C. The injector ensures an approximate output flow of kerosene of 2.5 GPH ($2.10 \times 10^{-3} \text{ L.s}^{-1}$). The ignition of the kerosene/air mixture is ensured by means of a spark plug fixed on the upper part of the cone located at the outlet of the burner (see Figure 2). During the experiments, the composite sample is placed at 100 mm from the outlet of the burner cone in a sample holder equipped with a deflector to avoid any flame bypass (see Figure 2). **The flame temperature is measured by a rack of seven K-type thermocouples having diameter of 1/8 inch positioned at the same spot as the test sample (100 mm from the burner cone), 20 mm apart from each other, and 25.4 mm above the central axis of the cone burner**

To deepen the understanding of composites' fire behavior, instrumentation available for the study of the degradation of composites has been employed. The mass loss of the composite

sample is measured using a SCAIME AG3 center support load cell located under the sample holder (see Figure 2). The maximum mass supported by the sensor is 50 kg with approximate uncertainty of 5 g, depending on the accuracy of the weighing sensor. **Considering a sample mass between 650 and 900 g a global uncertainty of 1 % with a confidence level of 95 % is used.** To ensure the validity of the mass loss measurement, the initial and final masses of all the samples are measured using a different scale. A Flir ThermCam PM 595 thermal imaging camera placed at the backside of composite, approximately 2.5 m from the sample providing an entire view of backward face is used to measure the temperature of the backside of composite samples during experiments. . The emissivity of the plate is considered as fixed and equal to 0.9 for the duration of the measurement [26], **resulting in a global uncertainty of 5 % with a confidence level of 95 %.**

3. Results and discussion

3.1. Experimental observations

The photographs in Figure 3 illustrate different phenomena observed during the cone calorimeter experiments performed with the horizontal configuration for the three composites studied. The four photographs present in Figure. 3 correspond to different characteristic times encountered during the tests. These characteristic times are the initial time ($t = 0$ s) where the test starts, the ignition time, $t = t_{ig}$ (approximately 20 seconds for carbon-phenolic, 25 seconds for carbon-PEKK and 30 seconds for the carbon-BMI) and the time when the rate of heat generation is maximum ($t = MAX_{HRR}$) and the time at the end of which the degradation reaction is terminated. The time for a maximum HRR can be different for each material (40s for BMI, 38s for the carbon-phenolic and 45s for the carbon-PEKK). Thus, for the carbon-phenolic sample, from the beginning of the test until $t = t_{ig}$, no flame is visible on the surface of sample and its temperature increases gradually. Once the degradation temperature of the resin is reached, decomposition starts, and the volatiles start getting accumulated on the

surface of the material. Once the concentration of the pyrolysis gases at the surface is sufficient and the temperature reaches the auto-ignition temperature, the mixture self-ignites (these condition might be promoted by the cone resistance). It was observed that eventually from a certain time (about 120s for carbon-phenolic, 140s for carbon-PEKK and 140s for carbon-BMI) no flame is visible on the surface of the two materials. This extinction can be caused by the accumulation of char on the surface of the sample preventing the diffusion of the pyrolysis gases [24]. A slight expansion of the sample at its surface is also observed. This is probably due to the accumulation of gas between the plies of the composite, caused by the degradation of the resin. Once the resin is largely degraded in the upper (thus porous) laminate ply, these gases are transported to the surface. While comparing the photographs for carbon-PEKK and phenolic carbon at the time of ignition ($t = t_{ig}$), it was noticed at the time of inflammation that unlike carbon phenolic which has an intense flame at its surface, the carbon-PEKK sample has a set of small flames located at different positions on the surface of the sample

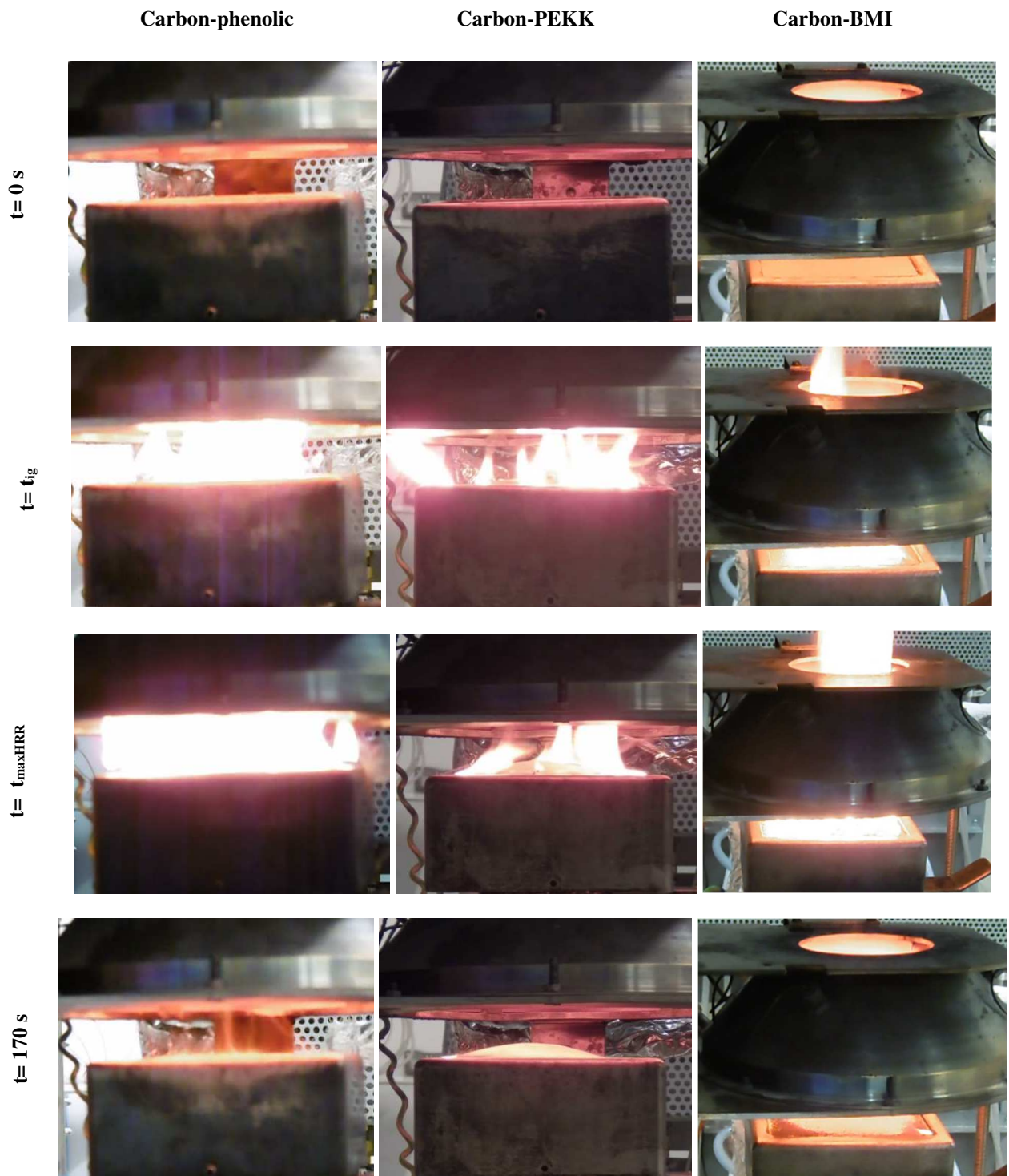


Figure 3. Photographs of the main events during cone calorimeter exposition for the three composites materials (horizontal configuration).

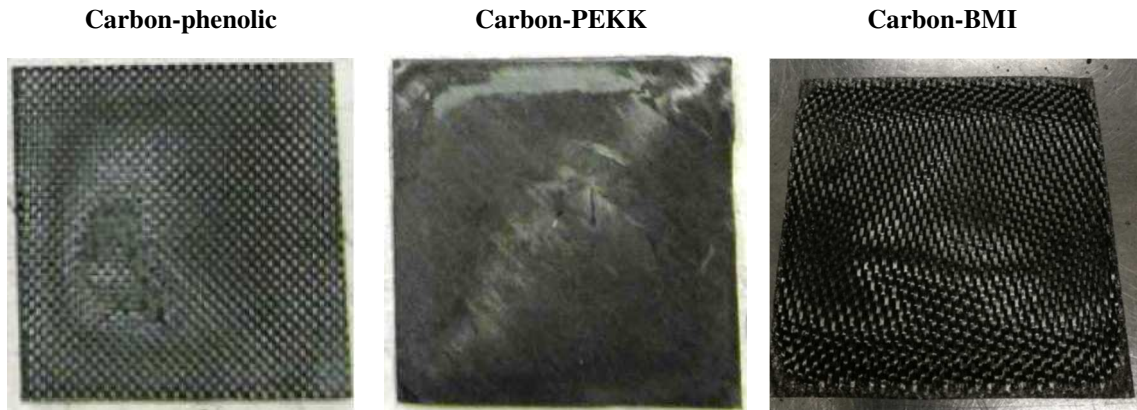


Figure 4. Photographs of the different composite samples after cone calorimeter experiments (vertical configuration –face exposed to heat flux)

Figure 5 shows three composites samples before their thermal degradation (5-a) as well as their front faces (5-b) and backward face (5-c) after being subjected to the NexGen burner flame for 15 minutes (under the standard temperature conditions). The exposed face of the carbon-PEKK sample has been significantly degraded by the flame in the center of the first ply of both resin and carbon-fiber. A weaker zone on the second ply seems degraded. It is interesting to note that the same level of degradation was observed during cone calorimeter tests (cf. figure 4). This significant consumption of carbon fibers on the first two plies reflects the presence of oxidizing phenomenon, probably due to the presence of a lean flame condition (i.e. presence of oxygen in the products of combustion). Regarding the front face, it has a large area (all around the degraded zone) where the partially degraded resin has undergone recrystallization during the cooling phase of the sample (solidification of the resin). This phenomenon is interesting in a real case, because it could provide better mechanical strength after the fire event, thus limiting risks of rupture. This behavior is one of the major advantages of thermoplastic composites compared to thermosetting composites and has been highlighted by Vieille *et al.* [27] and Maaroufi *et al.* [28]. On the back side, the resin seems less degraded and **the initial mechanical properties of the material can be preserved.**

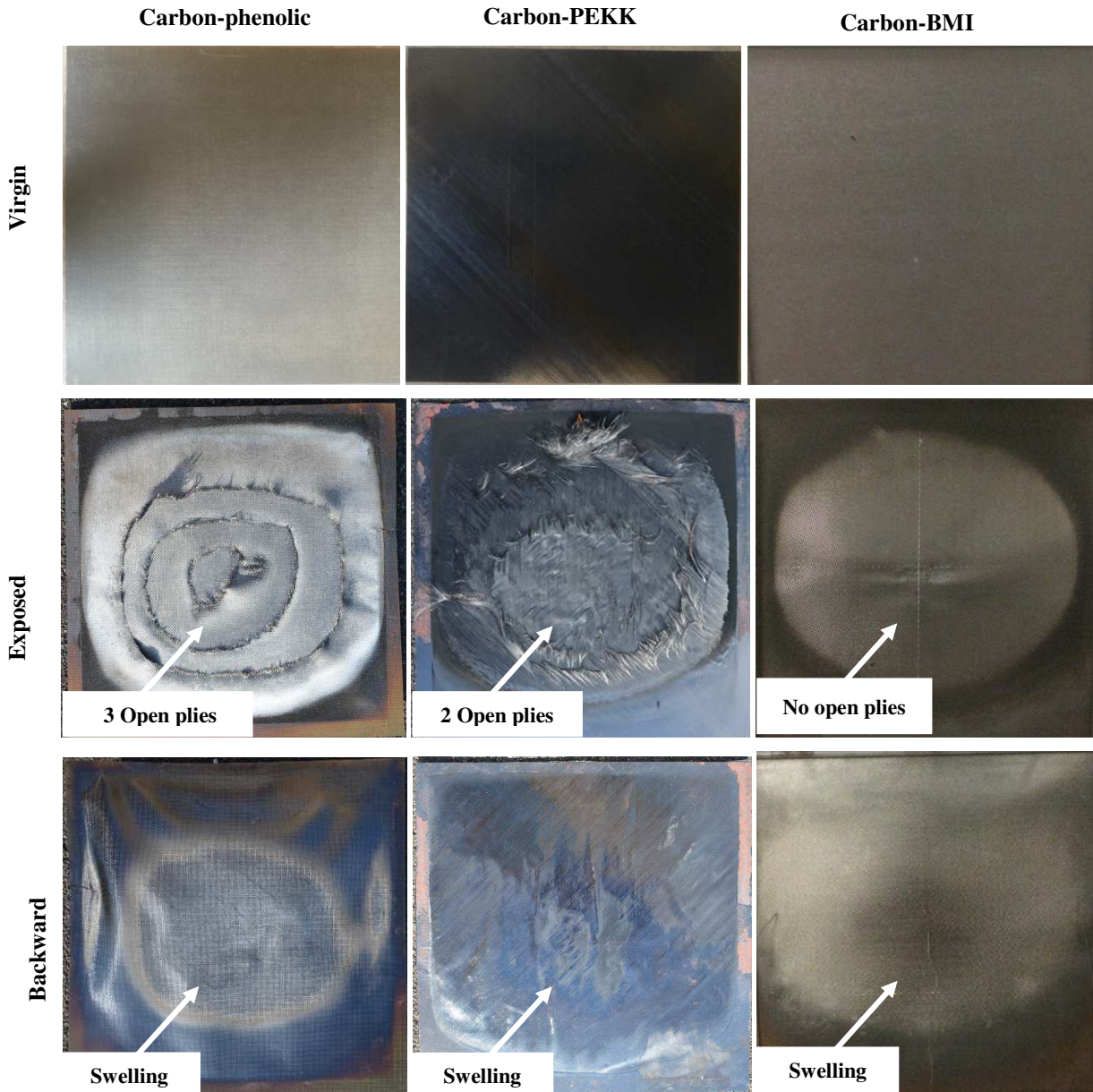


Figure 5. Photographs of the different composite samples before and after NexGen burner experiments. Since the degradation temperature of the carbon-PEKK is around 500 ° C [22], this observation suggests that the maximum temperature encountered at the rear face is approximately equal to this value. A slight swelling of the sample is also visible on the degraded sample, suggesting that a slight build-up of gas from pyrolysis of the resin occurred during the test or the residual mechanical constraint from the polymerization process. For the carbon-phenolic sample, the front face presents a significant degradation of the first 3 plies of the material (the same phenomenon was observed on the different samples tested). In

addition, a large amount of resin seems degraded; hence the structural strength of the material is decreased. This large amount of degraded carbon fiber can be explained by the presence of oxygen in the phenolic resin [29]. During the first degradation reaction of the resin, associated with its dehydration (between 100 °C and 300 °C) [7, 30], the oxidizing pyrolysis gases might promote the combustion of the carbon fibers. In addition, the greyish color of the composite surface seems to be associated with a significant presence of char. The back face of the sample presents an important amount of degraded resin with significant swelling of the surface leading to an important decrease of the structural integrity.

Contrary to two other materials, the carbon-BMI sample presents no open ply on its exposed surface, with an important amount of degraded resin. This suggests that the carbon fibers have not been oxidized during the decomposition due to a lower temperature or an insulation of the char produced during the pyrolysis of resin. A significant swelling of the exposed surface is also visible on the center of the sample, which might be due to a significant build-up of gases during the pyrolysis, which remained blocked by the non-degradation of the exposed surface. Nevertheless, the backside face of the sample present also a swelling of the surface suggesting that a slight build-up of gas from pyrolysis of the resin occurred during the test. However, contrary to carbon-phenolic, the resin at the surface of the backside face presents less important decomposition level.

3.2. Experimental mass loss

The experimental mass loss obtained for the different materials, **at both medium and large scales in a vertical configuration are presented on Figure 6.**

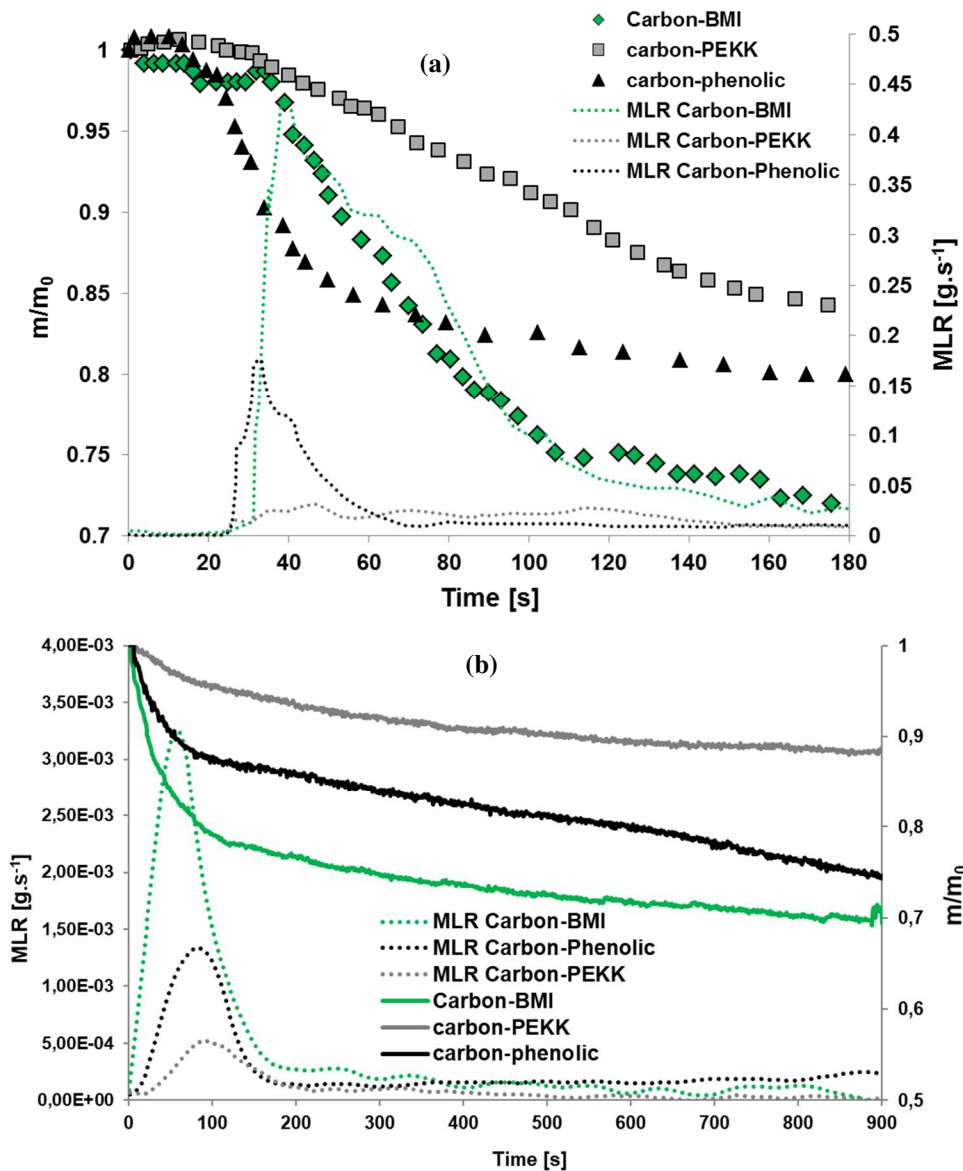


Figure 6. Mass loss measurement on the different composites samples at medium scale (a) and large scale (b).

At medium scale, for the carbon-PEKK, the mass loss demonstrates similar evolution. The mass is constant first up to 30 s, corresponding approximately to the ignition time, then a monotonous mass loss is observed until 160 s and then it starts to stabilize. The obtained final mass loss equals 15 % of the virgin sample mass. For the carbon-phenolic sample, different phases observed are visible. Initially, for almost 20 s (approximately the ignition time) the mass loss slightly changes, then an important and rapid mass loss between 20 s and 50 s is visible, and finally the mass loss decreases after 50 s until 23 % of the virgin sample mass was consumed. Finally, the carbon-BMI presents a mass loss like the one of the carbon-

phenolic. A first stage with a quasi-constant mass until 35 s is followed by a significant mass loss between 35 s and 110 s, and a monotonous mass loss after 110 s which concluded after 180 seconds, and a final mass loss of 28 % is found.

The differences observed in the mass loss behavior between the three materials are due to the nature of their resins. Moreover, the good thermal stability and the high melting point [20] [31] of the PEKK resin characterize its decomposition by a high yield of stable carbonaceous char (approximately 60 % of the original resin mass at small scale [20]) which bring a superior flammability resistance [32]. The thermoset phenolic and BMI resin decomposition involves an important mass loss due to scission reactions between units along the polymer chain [29]. These reactions are respectively around 300°C and 400 °C (corresponding to the second mass loss stage in Figure 6). The third stage of thermoset phenolic resin mass loss corresponds to the fusion of aromatic rings into carbonaceous char inducing superior fire performances and resulting in less mass loss rate than at the second stage [33]. However, contrary to both carbon-PEKK and carbon-phenolic, the carbon-BMI degradation does not involve degradation on the surface of the sample. Indeed, no open plies are visible despite important resin decomposition. This behavior might result in an interesting post fire mechanical behavior despite the important mass loss during the fire exposure. **Moreover, the differences in the degradation behavior between vertical and horizontal configuration have been discussed in a previous work [34].**

At large scale, the evolution of the mass loss is slightly different for the three materials. For the carbon-phenolic composite during their exposure to the NexGen burner flame (with an average initial mass of approximately 595 g), the loss of mass does not show significant variations between the three samples ensuring the reliability of the large-scale experiments in each run. The carbon-phenolic samples are characterized by a two-phase mass loss curve. The first phase starts as soon as the material is exposed to the flame and it continues for about

100 s, during this period, a mass loss of about 13% is reached (corresponding to about 77 g). This significant loss of mass, as soon as the material is exposed to the flame, can be associated with the rapid degradation of the resin being present on the surface of the material and causing the material temperature to increase rapidly over the first plies of the composite sample. This behavior is also validated by Biasi [34], who demonstrate that the characteristic chemical time is less important than the characteristic thermal conduction time, which confirms this hypothesis. For the rest of the fire exposure, the thermal phenomena are more evident and a thermal equilibrium is created between the front face and the rear face of the composite, leading to a decrease in the MLR, corresponding to the second phase. The mass of the sample then decreases monotonically until the end of the test and the final mass loss obtained is than of the order of 26% of the initial mass. As for the carbon-phenolic, the mass loss of the carbon-PEKK samples can be divided into two distinct phases. During the first phase, at the beginning of the test, an average mass loss of 6%, i.e. approximately 45 g, is obtained (see Figure 6.b). It is interesting to note that this phase lasts also approximately 100 s. The behavior of the two samples differs for the rest of test. The mean total mass loss obtained after 15 minutes for carbon-PEKK is approximately 11% of the initial mass. The smallest mass losses obtained for carbon-PEKK compared to that of carbon-phenolic can be explained by the better thermal stability of carbon-PEKK with thermal degradation starting around 500 °C [22]. In addition, the carbon-PEKK has a thermal conductivity lower than that of carbon-phenolic, between room temperature and 600 °C [17] thus limiting the diffusion of heat in the material, and therefore its degradation. Finally, as for the other two materials, the carbon-BMI presents a mass loss behavior divided into two phases with a first phase also during the first 100 s of the test. However, during this first phase the obtained mass loss is more evident with a value of approximately 23 %. **This important mass loss has been noticed at small scale by Faraz et al. [36] and the rapid mass loss might be explained by the catalyst**

role of the carbon fiber accelerating the decomposition due to the presence of iron particulates. For the rest of the test, the mass loss rate shows less change with a final mass loss of 28% (after 15 minutes). This behavior might be explained by the important charring behavior of the BMI resin as mentioned by Liu et al. [24]. It can be noticed that, over the first seconds of the test an important decomposition of the resin operates then the resin induces the production of an insulating layer at the surface of the sample, which limits the degradation during the rest of the test and limits also the plies opening, as mentioned previously. Nevertheless, the carbon-BMI presents more important mass loss compared to the two other materials.

By comparing the experimental mass losses at both medium and large scale, it appears that the final mass of the two tests are of the same order (despite tests with different duration) highlighting the lower front face temperature of the flame compare to the cone calorimeter. In both cases the carbon-PEKK presents less mass loss than the carbon-BMI. However, the evolution is different, because at medium scale no mass loss is observed during the first 40 seconds of the test (almost until the ignition of the exposed surface) whereas at large scale a mass loss is visible without any latency. This highlights the importance of resin degradation and oxidation in occurrence of a flame. Nevertheless, the cone calorimeter experiments on medium scale samples are representative of large-scale experiments regarding the mass loss behavior. Regarding the differences in samples degradation, this highlights the more aggressive degradation of the NexGen burner despite a less important front face temperature.

3.3. Experimental back face temperature

At medium scale, the average temperature profiles measured on the back faces are presented in Figure 7.a. The values correspond to the mean temperature measured, using infrared thermography, on a 40 x 40 mm zone in the center of the backward face of the samples.

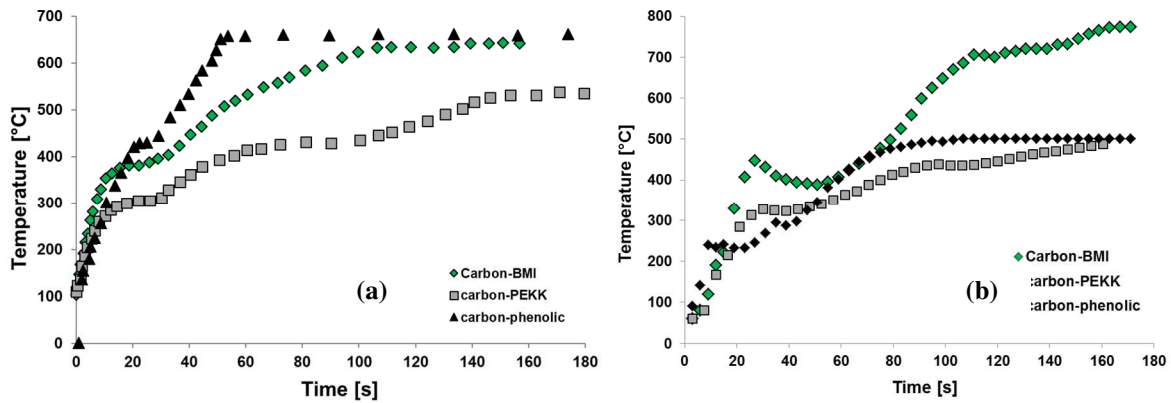


Figure 7. Temperature curves obtained with cone calorimeter (a) and NexGen burner (b) experiments.

For the three materials the temperature evolution can be divided into two phases, a transient one with a quick increase of the BFT (Backward Face Temperature) followed by a constant growth of the temperature.

For the carbon PEKK, two phases are visible in the temperature curves. The first phase presents a fast increase of the temperature between 0 and 30 s followed by a short stabilization (at about 300 °C) before a second temperature increase between 30 s and 90 s (of approximately 100 °C), Whereas Between 90 s and 180 s a final growth of approximately 100°C is observable. The latter can be associated with the stable phase. Regarding the carbon-phenolic sample, within the first 30 s the temperature raises 450 °C before increasing again over 650 °C which is the saturation temperature of the used infrared camera. Therefore, the final exact phenolic sample stabilization temperature has not been measured. Finally, the carbon-BMI samples also present a temperature evolution divided into three phases, between 0 and 20 s, the temperature increases from ambient to approximately 400 °C, then the BFT rises again up to 600 °C between 20 and 100 s to finally stabilize around 650 °C.

For the NexGen burner experiments, the average temperature evolution of a 1 cm x 1 cm area (i.e. a square of 4 pixels), located at the center of the rear face of the different samples, is computed for the totality of the test (15 minutes) and plotted on the Figure 7.b. It is interesting to note that the overall change in temperature for both materials is similar. The temperature evolution can be split into two phases. A first phase corresponding to the rise in temperature,

between 0 s and 150 s, presented on the figure 7.b, this phase might be associated with the significant degradation step visible on the MLR curve (figure 6.b). In second phase, the temperature remains almost constant (between 150 and 800 seconds). The slight change in temperature during this second phase agrees with the hypothesis put forward above, indicating that a thermal equilibrium is created in the material between the front face exposed to the flame and the rear face. At the same time, almost constant temperature leads to the very slow degradation of the composite observed on the mass loss curve. Contrary to the cone calorimeter experiments, the maximum temperatures obtained on the rear face of the materials are approximately equivalent, with temperatures between 500 °C and 550 °C **except for the carbon-BMI with higher temperature, up to 700 °C**. For the carbon-PEKK sample, whose onset of degradation is at around 500 °C [7], the maximum rear face temperature of around 550 °C justifies low degradation of the sample observed on the photograph of Figure 5. This phenomenon probably reflects the appearance of an insulation layer (resulting from the degradation of the resin on the surface of the composite). Meanwhile, the carbon-PEKK temperature tends to increase slightly. This increase in temperature is probably due to the opening of a fabric ply on the surface of the composite, resulting in a decrease in thickness of the material and therefore a higher thermal conductivity. The evolution of the temperature for the first 160 s of the tests is, in turn, visible in detail in figure 7.b for the three composites studied.

As observed during the cone calorimeter tests, the temperature evolution of the carbon-PEKK backward face has two points of inflection. A first point is visible at about 330 °C. This inflection of the temperature curve is probably associated with the melting of the resin as mentioned previously for the cone calorimeter experiments. The second inflection point, visible between 450 °C and 500 °C, probably reflects the beginning of the degradation of the front face of the samples resulting **in the production of char during the resin degradation**

coming to isolate the front face of the material. For carbon-phenolic, a single point of inflection is visible between 250 °C and 300 °C. As observed for the carbon-PEKK, this point might be associated with the beginning of the degradation reaction of the phenolic resin [7] leading to the production of char coming having an insulating role. Unlike carbon-PEKK, this inflection point was not as visible on the cone calorimeter tests. It is possible that **the combustion products** of the flame in comparison with the atmosphere environment during cone calorimeter testing is put forward this phenomenon.

Regarding large scale experiments, the temperature fields were measured using the infrared camera placed approximately 2.5 m from the back of the samples. Figure 8 presents instantaneous temperature field of the backward face of the carbon-PEKK sample after about 150 seconds of exposure to the flame. By comparing these photographs of the back of the materials, it is possible to notice that the hottest areas visible in the figure correspond roughly to the most degraded areas visible in Figure 8. It is in these areas that the carbon fibers begin to oxidize leading to opening in the first plies on the carbon-PEKK and carbon-phenolic samples.

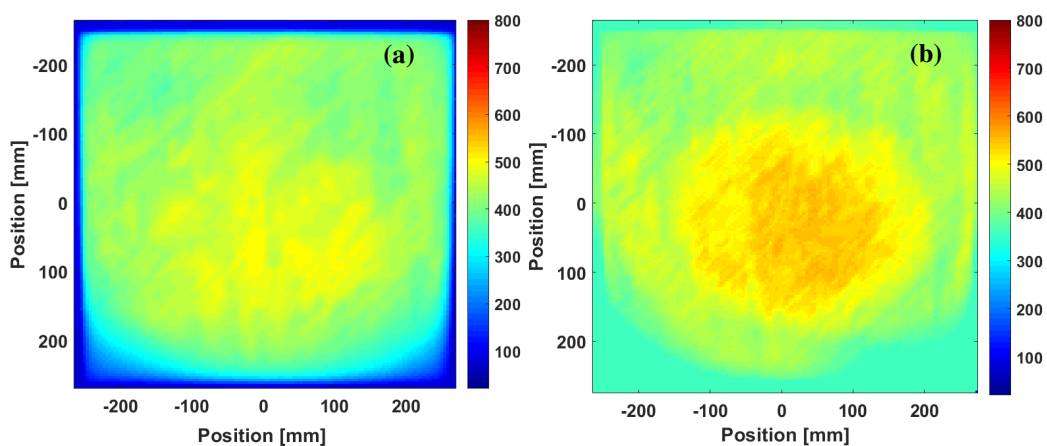


Figure 8. Temperature visualization for large scale samples after 200 seconds (a) and after 800 seconds (b) for the carbon-PEKK.

As demonstrated with the mass loss, the experimental backward face temperature measured at meso-scale and large scales present the same behavior **with a transposition of the different phenomena between the different scales.** In spite of that a less changing temperature is

measured during the NexGen Burner experiments; which indicates that, despite the same heat flux range used to decompose the materials, the thermal exposure is different. Indeed, in Figure 7b it is shown that there are very similar back face temperatures for PEKK carbon and BMI carbon evolutions, but there is an important difference for carbon phenolic (600 ° C for cone calorimeter test and 400 ° C for NexGen burner test) and carbon BMI where the maximum temperature reach 800 °C. for the carbon-Phenolic, this difference can be explained by the high swelling and delamination of the composite plies during the test inducing thermal insulation **by an internal gas zone**, it is observed that the initial slope is identical for the 2 experiments, but the evolution obtained from burner is broken in the very first seconds **(between 20 s and 40 s)** probably by a first delamination or swelling of the internal ply of the test panel **reducing the heat transfers during the decomposition**. Moreover, this phenomenon was not observed significantly for cone calorimeter test. For the carbon-BMI, this large increase of **temperature at the end of the test** might be explain by **the catalyst role of the carbon fiber accelerating the resin decomposition, as explain before, which can lead to an increase of temperature as less resin is present in the materials**

3.4. Experimental Heat Release Rate

Figure 9 presents the Heat Release Rate (HRR) measured at medium scales and the HRR for large scale is calculated using mass loss rate and heat of combustion [35] measured at large scale. **For the carbon-BMI composite, The HRR values presented at large scale are calculated from the Heat of combustion calculated with the total Mass loss and the total Heat Release Rate obtained at medium scale with the cone calorimeter experiments.**

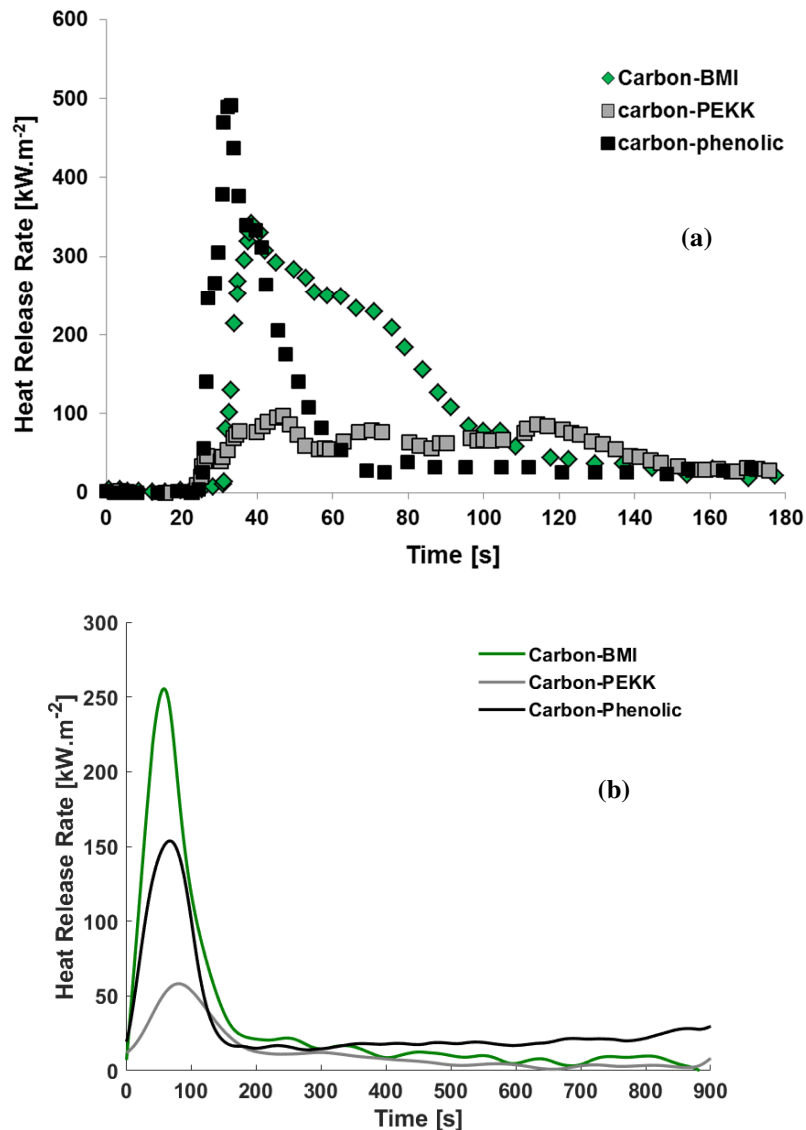


Figure 9. Heat Release Rate curves obtained with cone calorimeter (a) and NexGen Burner (b) experiments.

At medium scale the experimental HRR (horizontal configuration) for the three materials demonstrate the difference in the decomposition process among the materials. While comparing the results of the three composites for HRR in horizontal configuration, the carbon-phenolic presents a rapid increase of the HRR 540 kW/m^2 . The latter is caused by scissions in the main polymer chain generating an important amount of flammable volatiles such as methane, ethane, carbon monoxide and hydrogen [36, 23], thus increasing the flammability of the composite. At the same time, the fusion of the aromatic rings leads the formation of carbonaceous char layer on the surface causing a rapid decrease of the HRR to a constant value of 60 kW/m^2 . On the other hand, the carbon-PEKK presents a maximum HRR

values of approximately 100 kW/m² with a larger peak presenting oscillation within a range of 20 kW/m² which might correspond to the flame oscillation on the surface, after that HRR values are decreasing down to 35 kW/m² at 160 s and seems to remain constant till the end of the test. This lower value of HRR might be caused by a decrease of the flammable volatiles [37, 23] leading to a decreased value of HRR. Once the resin is decomposed, the HRR of each material decreases to a residual value, which corresponds to the combustion of the char and the fibers [37]. Finally, The Carbon-BMI present an intermediate behavior with a large peak and a maximum value of 350 kW/m² at 45 s decreasing to approximately 40 kW/m² around 120 s. It is observed in Figure 3 that in each case after 160 s, no more flame is visible on the surface of the three composites, which indicates that internal heat generation process occurs [38] probably associated with the resin decomposition in the internal plies or the carbon fiber combustion on the surface of the sample.

At large scale, the HRR of the three materials present a first period of rapid degradation at the beginning of the test is visible, with a peak on the curve (between 0 and 100 s). It is interesting to note that the maximum value of the HRR for all the materials is obtained at around 100 s with a maximum value of approximately 160 kW/m² for the carbon-phenolic and 50 kW/m² for the carbon-PEKK. For the second period (between 100 s and 900 s) the HRR shows a different evolution between the two materials. The HRR of the carbon-PEKK and the carbon-BMI slowly decreases to a value close to zero, whereas for carbon-phenolic the HRR is almost constant until the end of the test (explaining the constant mass loss observed on the Figure 6). While Comparing the HRR obtained at medium and large scale, one can observe the evident difference in the HRR behavior. At large scale, the materials exhibit similar behavior when exposed to fire of difference intensities, and the calculated values of HRR are lower. Nevertheless, the material classification is conserved with a lower

HRR for the carbon-PEKK, highlighting its superior fire behavior compared to the carbon-phenolic.

4. Conclusion

In the present study, the fire behavior of three carbon-reinforced composites has been evaluated experimentally at medium and large scale. The experimental characterization performed at both scales gives an insight to different phenomena, and based on these phenomena various results have been observed and explained.

The mass loss behavior obtained at medium and large scale demonstrates that the carbon-PEKK composite presents a superior thermal stability with a less change in temperature and a moderate backside face temperature. Moreover, this material presents a limited HRR value up to five times less than that of carbon-phenolic and three times less than that of carbon-BMI, thus limiting the fire spread. In the same manner, for both scales the temperature measures performed on the backside face demonstrate a similar behavior. Although, there are very similar back face temperatures for PEKK carbon and BMI carbon, but there is a big difference for carbon phenolic. The high swelling and delamination of the composite plies can explain this difference during the test inducing thermal insulation by a created space. These experimental results for the three materials demonstrate that both experimental scales give similar results despite the difference in the sample scale and thermal exposition (radiative vs flame). This similarity of the phenomena observed for the two-studied scale reveals the ability of the meso-scale experiments to provide a precise overview of the fire behavior of a material before performing large scale experiments in order to reduce the number of tests and consequently the developmental costs.

Acknowledgment

I am particularly grateful to Mrs. Madiha Rashid* for generously giving her time to review the paper. Her efforts in improving and clarifying the subject matter are much appreciated.

References

- [1] G. Marsh, "Bombardier throws down the gauntlet with Cseries airliner," *Reinforced Plastics*, vol. 55(6), pp. 22-26, 2011.
- [2] Y. Shi, T. Swait and C. Soutis, "Modelling damage evolution in composite laminates subjected to low velocity impact," *Composite Structures*, vol. 94 (9) , pp. 2902-2913, 2012.
- [3] J.-S. Kim, J.-C. Jeong and S.-J. Lee, "Numerical and experimental studies on the deformational behavior a composite train carbody of the Korean tilting train," *Composite Structures*, no. 81, pp. 168-175, 2007.
- [4] G. Marsh, "Airbus takes on Boeing with reinforced plastic A350 XWB," *Reinforced plastics*, vol. 51(11), pp. 26-29, 2007.
- [5] E. R. Fuchs, F. R. Fields, R. Roth and R. E. Kirchain, "Strategic materials selection in the automobile body: Economic opportunities for polymer composite design.," *Composites Science and Technology* , vol. 339(6119), pp. 1989-2002, 2008.
- [6] M. F. De Volder , S. H. Tawfick , R. H. Baughman and A. J. Hart, "Carbon nanotubes: present and futur commerical applications," *Science*, vol. 339 (6119), pp. 535-539, 2013.
- [7] A. P. Mouritz and A. G. Gibson, *Fire properties of polymer composite materials*, Dordrecht: Springer Science & Business Media , 2007.
- [8] N. Grange, K. Chetehouna, N. Gascoin and S. Senave, "Numerical investigation of the heat transfer in an aeronautical composite material under fire stress," *Fire Safety Journal* , vol. 80, pp. 56-63, 2016.
- [9] International Standard, *Aircraft environmental test procedure for airborneequipment resistance to fire in designated fire zones*, 1998.
- [10] Federal aviation administration , *Powerplant installation and propulsion system component fire protection test methods, standard and criteria*, US Department of transportation , 1990.
- [11] J. Zhang, X. Wang, F. Zhang and A. R. Horrocks, "Estimation of heat release rate for polymer-filler composites by cone calorimetry," *Polymer Testing*, vol. 23 (2), pp. 225-230, 2004.
- [12] F. Y. Hshieh and H. D. Beeson, "Flammability testing of flame-retarded epoxy composites and phenolic composites," *Fire and Materials* , vol. 21(1), pp. 41-49, 1997.
- [13] A. Genovese and R. A. Shanks, "Fire performance of poly (dimethyl siloxane) composites evaluated by cone calorimetry," *Composites Part A: applied science and manufacturing* , vol. 39(2), pp. 398-405, 2009.
- [14] International Standards, *Reaction to fire tests. Heat release, smoke production and mass loss rate part 1 : Heat release rate (Cone calorimeter method)*, 2002.
- [15] T. Fateh, T. Rogaume and F. Richard, "Multi-scale modeling of the thermal decomposition of fire retardant plywood," *Fir safety Journal*, vol. 64, pp. 36-47, 2014.
- [16] S. Feih, Z. Mathys, G. Mathys, A. G. Gibson, M. Robinson and A. P. Mouritz, "Influence of water content on failure of phenolic composites in fire," *Polymer degradation and stability* , vol. 93(2), pp. 376-382, 2008.
- [17] N. Grange, P. Tadini, K. Chetehouna, N. Gascoin, S. Senave and I. Reynaud, "Determination of thermophysical properties for carbon-reinforced polymer-based composites up to 1000°C," *Thermochemica Acta*, vol. 659, pp. 157-165, 2018.
- [18] U. Sorathia , C. M. Rolhauser and W. A. Hughes, "Improved fire safety of composites for naval applications," *Fire and Materials* , vol. 16(3), pp. 119-125, 1992.
- [19] K. Chetehouna, N. Grange, N. Gascoin, L. Lemée, I. Reynaud and S. Senave , "Release and flammability evaluation of Pyrolysis Gases from carbon-based composite materials undergoing fire conditions," *Journal of Analytical and Applied Pyrolysis*, 2018.
- [20] P. Tadini, N. Grange, K. Chetehouna, N. Gascoin, I. Reynaud and S. Senave, "Thermal degradation analysis of innovative PEKK-based carbon composites for high-temperature aeronautical components," *Aerospace Science and Technology*, vol. 65, pp. 106-116, 2017.
- [21] J. Fink, *Reactive Polymers Fundamentals and Applications : A Concise Guide to Industrial Polymers*, Norwich, NY, USA: William Andrew Publishing, 2005.
- [22] Y.-L. Liu and Y.-J. Chen, "Novel thermosetting resins based on 4-(N-maleimidophenyl)glycidylether: II. Bismaleimides and polybismaleimides," *Polymer*, vol. 45, pp. 1797-1804, 2004.
- [23] L. Riviere , N. Causse, A. Lonjon, E. Dantras and C. Lacabanne, "Specific heat capacity and thermal conductivity of PEEK/Ag nanoparticles composites determined by Modulated Temperature Differential Scanning Calorimetry," *Polymer Degradation and Stability* , vol. 127, pp. 98-104, 2016.

- [24] E. S. Oztekin , S. B. Crowley, R. E. Lyon, S. I. Stoliarov, P. Patel and T. R. Hull, "Source of variability in fire test data: A case study on poly(aryl ether ether ketone)(PEEK)," *Combustion and Flame*, vol. 159(4), pp. 1720-1731, 2012.
- [25] V. Babrauskas, "Development of the cone calorimeter-a bench scale heat release rate apparatus based on oxygen consumption," *Fire and Materials*, vol. 8 (2), pp. 81-95, 1984.
- [26] E. Schuhler, A. Coppalle, B. Vieille, B. Yon and Y. Carpier, "Behaviour of aeronautical polymer composite to flame: A comparative study of thermoset-and thermoplastic-based laminate," *Polymer Degradation and Stability*, vol. 152, pp. 105-115, 2018.
- [27] B. Vieille, C. Lefebvre and A. Coppalle, "Post fire behavior of carbon fibers polyphenylene sulfide and epoxy-based laminates for aeronautical applications : A comparative study," *Materials&Design*, vol. 63, pp. 56-68, 2014.
- [28] M. Maaroufi, Y. Carpier, B. Vieille, L. Gilles, A. Coppalle and F. Barbe, "Post-fire compressive behavior of carbon fibers woven-ply Polyphenylene Sulfide laminates for aeronautical applications," *Composites Part B: Engineering*, vol. 119, pp. 101-113, 2017.
- [29] A. Knop and L. A. Pilato, Phenolic resins: Chemistry, applications and performance, Springer Science & Business Media, 2013.
- [30] H. Jiang, J. Wang, S. Wu, Z. Yuan, Z. Hu, R. Wu and Q. Liu, "The pyrolysis mechanism of phenol formaldehyde resin," *Polymer degradation and stability* , vol. 97, pp. 1527-1533, 2012.
- [31] P. Patel, T. R. Hull, R. W. McCabe, D. Flath, J. Grasmeyer and M. Percy , "Mechanism of thermal decomposition of poly (ether ether ketone)(PEEK) from a review of decomposition studies," *Polymer degradation and stability*, vol. 95(5), pp. 709-718, 2010.
- [32] H. W. Lochte, E. L. Strauss and R. T. Conley, "The thermo-oxidative degradation of phenol-formaldehyde polycondensates: Thermogravimetric and elemental composition studies of char formation," *Journal of Applied Polymer Science* , vol. 9 (8), pp. 2799-2810, 1965.
- [33] K. A. Trick, L. A. Saliba and S. S. Sandhu, "A Kinetic model of the pyrolysis of phenolic resin in a carbon/phenolic composite," *Carbon*, vol. 35(3), pp. 393-401, 1997.
- [34] V. Biasi, Modélisation thermique de la dégradation d'un matériau composite soumis au feu, Toulouse: Université de Toulouse, 2014.
- [35] R. Walters, S. Hackett and E. Lyon, "Heats of combustion of high temperature polymers," *Fire and Materials* , vol. 24(5), pp. 245-252, 2000.
- [36] K. A. Trick and T. E. Saliba, "Mechanism of the pyrolysis of phenolic resin in a carbon/phenolic composite," *Carbon*, vol. 33(11), pp. 1509-1515, 1995.
- [37] P. Patel, A. A. Stec, T. R. Hull, M. Naffakh, A. M. Diez-Pascual, G. Ellis and R. E. Lyon, "Flammability properties of PEEK and carbon nanotube composites," *Polymer degradation and stability*, vol. 97(12), pp. 2492-2502, 2012.
- [38] D. P. Macaione, "Flammability characteristics of fiber-reinforced epoxy composites for combat vehicle applications," *U.S Army Materials Technology Laboratory*.